JOURNAL OF CATALYSIS 75, 39–48 (1982)

Changes in the Surface Structure and Composition of an Iron Catalyst of Reduced or Unreduced Fe_2O_3 during the Reaction of Carbon Monoxide and Hydrogen

J. P. REYMOND, P. MÉRIAUDEAU, AND S. J. TEICHNER

Laboratoire de Catalyse Appliquée et Cinétique Hétérogène (L.A. No. 231 Associé au C.N.R.S.), Université Claude Bernard (Lyon I), 43 Boulevard du 11 Novembre 1918, 69622 Villeurbanne Cédex, France

Received January 12, 1981; revised November 24, 1981

Iron oxide (Fe_2O_3) prepared by decomposition of iron nitrate acquires a catalytic activity in the CO + H_2 (1 atm) reaction at 250°C even without any reduction pretreatment in H_2. The nonreduced catalyst and the reduced one have their surface and bulk compositions modified in different ways. In both cases the surface is covered by carbon and a small fraction of it is directly involved in the Fischer–Tropsch reaction with H_2, whereas the remainder is transformed into carbide not involved in the Fischer–Tropsch reaction or stays as inactive carbon. The formation of iron carbide is faster for the reduced sample and must be correlated with a higher rate of deactivation of this sample than of the nonreduced sample. A sequence of steps, different for the nonreduced and the reduced catalysts, is proposed, and accounts for the higher Fischer–Tropsch activity of the former material.

INTRODUCTION

It has been shown previously (*1*) that an iron catalyst in the form of α-Fe_2O_3 (unsupported) prepared by the thermal decomposition of hydrated iron nitrate is more active at 250°C in the CO + H_2 conversion after a mere heating in He instead of H_2 (that is, without a previous reduction) than a prereduced oxide, converted into α-Fe. It is therefore of interest to correlate this behaviour with the surface structure and composition of these two differently treated samples. In the case of silica-supported iron oxide (aerogel catalysts of surface area exceeding 700 m^2/g) the oxygen pretreatment leads to a 50-fold increase of the catalytic activity in the stationary state as compared to that of a prereduced catalyst (*2*). Moreover, no iron carbide nor metallic iron is found on the preoxygenated spent catalyst but only Fe_3O_4. The question which then arises is that of the nature of the active precursor of the catalyst, metallic iron and/or iron oxide. The identification of phases in the highly divided, supported, catalyst is more difficult than in the case of unsupported iron oxide precursor. This paper also deals with the unsupported catalyst, and the corresponding conclusions seem to be of a general value and apply as well to the highly divided, supported, iron oxide precursor (*2*).

EXPERIMENTAL

The catalytic activity in the CO + H_2 conversion and the hydrogen etching measurements of the catalyst after a given time on stream in Fischer–Tropsch conversion were studied in a differential microreactor equipped with a gas chromatograph (Porapak Q columns). X-Ray diffraction (XRD) patterns (Debye–Scherrer) were obtained on a Philips type PW 1009 diffractograph using a cobalt anticathode. The surface analysis (XPS) was made on a VG 3 spectrometer with an aluminium cathode, equipped with an argon gun for ion etching purposes. The catalyst was prepared by decomposition of $Fe(NO_3)_3 \cdot 9\ H_2O$ in air at 160°C (24 h) followed by baking in air at 200°C overnight. The XRD pattern of this precursor corresponded to that of α-Fe_2O_3 (*1*). This catalyst was used in the conver-

0021-9517/82/050039-10$02.00/0

sion of CO + H_2 either (i) without any reduction pretreatment in H_2 but after 30 min thermal pretreatment in He at 250°C (catalyst A), or (ii) after reduction in a hydrogen flow (60 cm^3 min^{-1}) during 15 h at 250°C. In case (ii) the XRD pattern was that of α-Fe (catalyst B). The CO + H_2 mixture (CO/H_2 = 1/9), with a flow of 60 cm^3 min^{-1} in the differential reactor, was converted by the Fischer–Tropsch reaction over 50 mg of catalyst A or B at 250°C, under 1 atm pressure.

RESULTS AND DISCUSSION

1. *Catalyst A (α-Fe_2O_3)*

The products of the reaction were C_1 to C_6 alkanes, CO_2, and H_2O (*1*). The selectivities for various alkanes remained almost constant during the run. After 5 h time on stream the composition of hydrocarbons was 40% C_1, 20% C_2, 20% C_3, 13% C_4, 6% C_5, and 2% C_6. Figure 1 gives the rate of formation of CH_4 (in micromoles CH_4 per minute and per gramme of initial Fe^{3+}) as a function of time on stream. The catalytic activity starts from zero and increases very rapidly, reaches a maximum after 5.5 h, and thereafter steadily decreases. The surface composition of the catalyst was studied (Fig. 1) after 1.5 h (point a), 5.5 h (point b), and 15 h (point c). For this purpose the temperature of the catalyst was sharply decreased from 250 to 25°C under the flow of CO + H_2; the sample was then removed from the reactor and transferred in air into the XPS spectrometer. This procedure was employed because the XPS instrument was not equipped with a reaction chamber. However, the exposure of iron catalysts to the laboratory atmosphere is not a serious drawback for the reliability of the results. Indeed, the XRD experiments which were performed after exposure to air of the reduced (H_2 at 250 or at 500°C) catalyst or without this exposure (direct reduction in the Guinier–Léné camera) gave the same results (the absence of iron oxides). A similar finding was reported in the Mössbauer spectroscopy experiments with silica-supported iron (*3*) where partially or fully reduced catalysts were found to be resistant

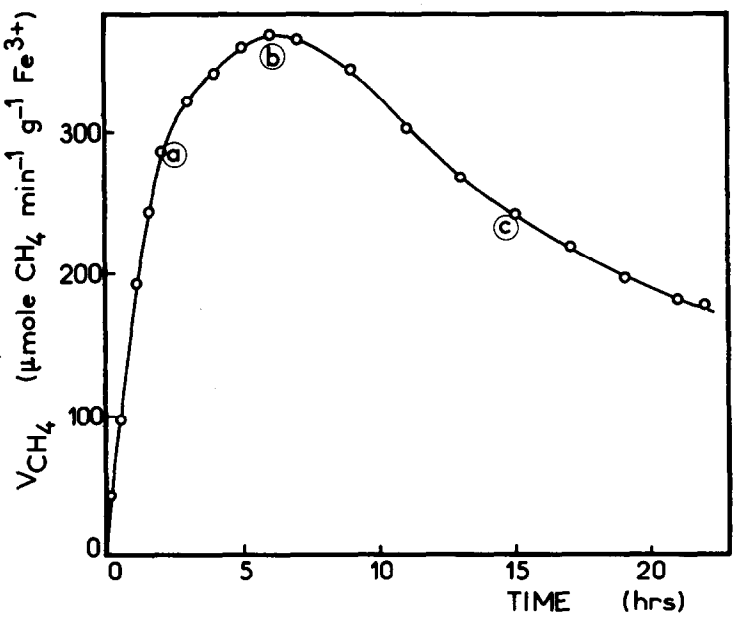

FIG. 1. Catalyst A (α-Fe_2O_3). Rate of formation of CH_4 in the Fischer–Tropsch conversion as a function of time on stream (in micromoles of CH_4 per minute and per gramme of initial Fe^{3+}).

TABLE 1

The Surface and Bulk Composition of Catalyst A (α-Fe_2O_3)

Time on stream of the Fischer–Tropsch reaction (Fig. 1)	Surface composition (XPS)[a] (arbitrary units)		Structure (XRD)	Hydrocarbons formed by H_2 etching (moles of CH_4 per atom of initial Fe^{3+})		
				250°C	500°C	Total
	Fe	C				
0	1 (710.8)	0.26 (284.8)	α-Fe_2O_3	0	0	0
(a) 1.5 h	1 (710.4)	0.95 (284.7)	*Fe_3O_4*[b] + χ-Fe_2C	0.21	0.028	0.24
(b) 5.5 h	1 (710.4)	1.25 (284.7)	Fe_3O_4[c] + χ-Fe_2C[c]	0.72	0.2	0.92
(c) 15 h	1 (710.3)	2.45 (284.7)	Fe_3O_4 + *χ-Fe_2C*	1.13	0.4	1.53

[a] The first number is related to the concentration, arbitrarily fixed at 1 for Fe and calculated by using cross sections published in (5), and has to be compared with the number relative to carbon (next column). The number in parentheses represents the binding energy in electron volts.

[b] The most abundant phase is italicized.

[c] In equivalent amount.

to oxidation on exposure to air at room temperature for several hours. Only a small amount of Fe_3O_4 (besides α-Fe) was found by Mössbauer spectroscopy after reduction (H_2 at 350°C) and handling in air of unsupported α-Fe_2O_3, whereas the XRD spectroscopy showed only the pattern of α-Fe (*4*).

The present XPS results are reported in Table 1 but no conclusion concerning the state of oxidation of iron is given as it is not needed for the present discussion. Fe (ionic or metallic) and C relative concentrations were calculated using the equation

$$\frac{n_1}{n_2} = \frac{I_1}{I_2}\frac{\sigma_2}{\sigma_1}\left(\frac{E_{k_2}}{E_{k_1}}\right)^{1/2}$$

where I_i is the intensity of the peak i, E_{k_i} the kinetic energy of this peak, σ_i the cross section calculated according to Ref. (5). The calibration of binding energies was performed by using the gold $4f_{5/2}$ line at 84 eV (5).

In a parallel series of experiments, for the same designated periods of time on stream as in Figs. 1a–c, the CO supply was terminated and only pure hydrogen flowed into the reactor. The formation of methane was monitored during this hydrogen etching and Fig. 2 represents the partial pressure of methane as a function of time. The total number of moles of methane formed after hydrogen etching at 250°C and then at 500°C is reported in Table 1. After hydrogen etching at 500°C, both catalysts A and B give an XRD pattern of α-Fe despite air handling of the samples. The pattern of iron oxides or carbides is not found. After hydrogen etching at 250°C catalyst A exhibits the XRD pattern of α-Fe, Fe_3O_4, and Fe_2O_3, whereas catalyst B remains in the reduced state (α-Fe). This behaviour shows higher activity versus oxygen from air of the unreduced (A) spent catalyst which has been treated by H_2 (etching). Table 1 shows simultaneously the surface composition (XPS) and the bulk structure (XRD). The surface carbon content (as measured by XPS) and the total carbon content (as measured by CH_4 formed by H_2 etching) increase (Table 1) with time on stream (a–c) of the Fischer–Tropsch reaction (Fig. 1). It

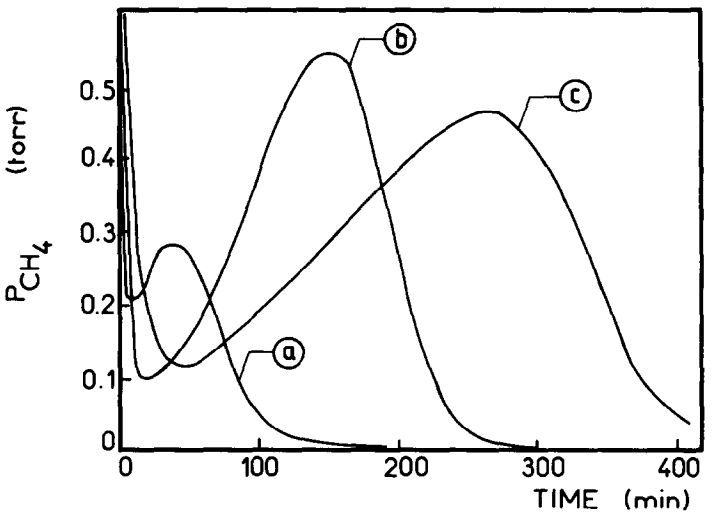

FIG. 2. Hydrogen etching forming methane at 250°C of catalyst A (α-Fe_2O_3) after Fischer–Tropsch conversion during 1 h 30 min (curve a), 5 h 30 min (curve b), 15 h (curve c).

has been shown previously (*6*) that virtually all carbon is removed by hydrogen (as CH_4) at 500°C and the structure of the catalyst is then that of α-Fe, but only a fraction of carbon is gasified at 250°C. It is also possible to distinguish the type of carbon generating methane in the hydrogen etching experiments of Fig. 2. The fast initial decrease of p_{CH_4} (C_2 and C_3 hydrocarbons are also formed) is due to the consumption by hydrogen etching of the active surface carbon which is the intermediate in the formation of hydrocarbons in the Fischer–Tropsch conversion (*7*). It explains the high reactivity of this carbon when compared with the reactivity in the next period of an increasing and then decreasing partial pressure of methane (Fig. 2) (no other hydrocarbons recorded) where this compound results from the reduction of iron carbide into CH_4 and α-Fe and the gasification of the less active carbon (*8, 9*). The binding energy of carbon (Table 1), of 284.7 (or 284.8) eV shows that the initial surface carbon is not in the form of iron carbide whose binding energy is lower (283.3 eV) but in the form of a graphitic carbon (*10*). An eventual formation of iron carbide below the initial surface of active carbon could be detected after an etching of the surface by argon ions, assuming that the composition of the surface is not qualitatively changed by etching. These experiments performed in the XPS spectrometer are reported in Table 2 and Figs. 3a and b, for catalyst A having been employed in the Fischer–Tropsch conversion during 5.5 h (point b of Fig. 1). Table 2 shows that the ratio C/Fe decreases with the number of etchings by argon ions.[1] This behaviour indicates that the surface concentration of carbon (noncarbidic carbon) is

TABLE 2

Surface Composition of Catalyst A after 5.5 h in Fischer–Tropsch Conversion as Revealed by XPS before and after Etching by Argon Ions

Number of etchings	C/Fe calculated as in Table 1	C 1*s* binding energy (eV)
0	1.2	284.7
1	0.9	284.7, 283.4
2	0.4	284.7, 283.4

[1] The C/Fe ratio found on pure reduced iron which was only in contact with air and then with the oil diffusion pump was found to be smaller than 0.1 with the C_{1s} value of 284.8 eV [graphitic carbon (*10*)].

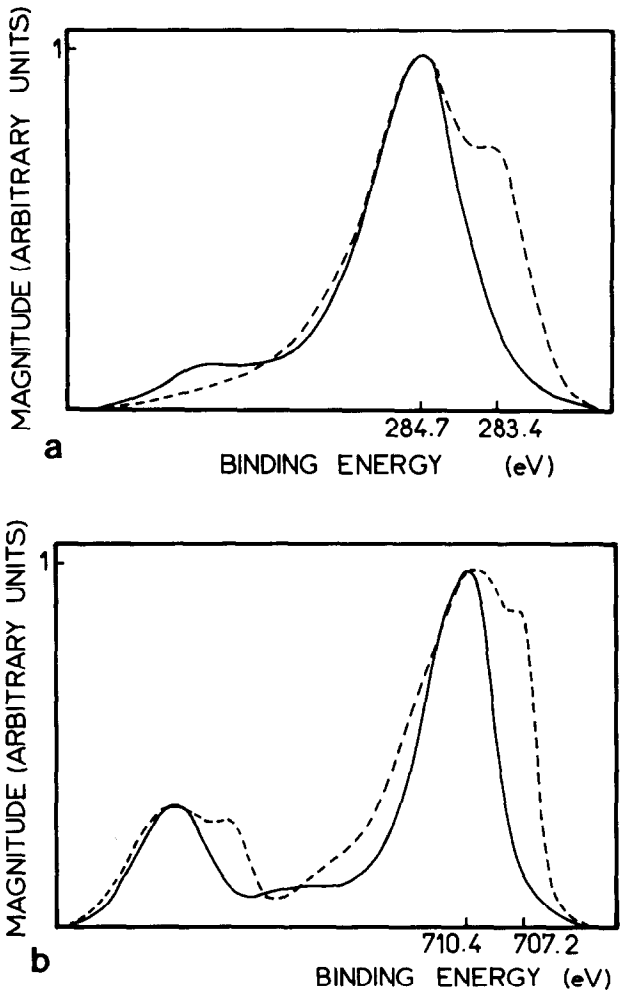

FIG. 3. Catalyst A (α-Fe_2O_3). (a) XPS measurements of the C 1*s* signal before (solid curve) and after (broken curve) etching by argon ions. The magnitude of the C 1*s* signal is normalized as 1 in the peak. (b) XPS measurements of the Fe $2p_{1/2}$ and $2p_{3/2}$ signals before (solid curve) and after (broken curve) etching by argon ions. The magnitude of the Fe $2p_{1/2}$ signal is normalized as 1 in the peak.

higher (before etching) than the bulk concentration (iron carbide) appearing after etching. Simultaneously the binding energy of surface carbon [284.7 eV, noncarbidic or graphitic (*10*)], observed before etching, decreases to 283.4 eV [carbidic (*10*)] after etching (Fig. 3a) which accounts for the incorporation of the bulk carbon into the iron carbide structure (*11*). In the same way Fig. 3b shows that the binding energy of iron decreases by etching from the value 710.4 eV, corresponding to the ionic iron (the spent sample is handled in air), to the value 707.2 eV which is that expected for iron in iron carbide (*11*). The Fe $2p_{3/2}$ values ranging (Fig. 3b) from 710.2 to 710.8 eV represent various degrees of oxidation of iron (*10*). They are not discussed here as the experimental conditions may not allow the conservation of the reduced state of iron. It is important to point out that the unreduced catalyst (α-Fe_2O_3) is in part converted into iron carbide (bulk) already after 1.5 h of Fischer–Tropsch conversion (Table 1) as shown by the XRD analysis but the greater fraction of the solid is converted

into Fe_3O_4. It is only after 15 h of conversion that iron carbide is the most abundant phase (Table 1). As the catalytic activity (as CH_4) decreases (Fig. 1b) when the formation of carbide in the solid phase increases it is inferred that iron carbide is not the intermediate in the Fischer–Tropsch conversion, as was already pointed out recently (*3*). This iron carbide can be converted by hydrogen etching at 250°C into methane only, whereas hydrogen etching of surface active carbon generates higher hydrocarbons as well (see above). It has been shown that the reduction of α-Fe_2O_3 into lower oxides and finally iron is a process of sequential steps, each phase being in equilibrium with the $CO-CO_2$ atmosphere (in the absence of H_2) (*12*). The reduction of Fe_2O_3 into Fe_3O_4 is fast whereas the conversion of Fe_3O_4 into FeO is much slower, but again the reduction of FeO into Fe is fast. On the other hand, the carburization of Fe must be a fast process as metallic iron is never detected (nor is FeO) by the XRD experiments of Table 1, the most stable phases during the reaction being Fe_3O_4 and iron carbide. Also the question which arises concerning the sequence of steps occurring with the unreduced catalyst during the conversion of a mixture of $CO + H_2$ is whether or not the metallic iron is required to produce the active carbon (generating CH_4 and homologues) formed by the dissociation of CO by the solid phase. It has indeed been shown that this dissociative adsorption may be the source of active carbon (*13, 14*):

$$CO + Fe_{(s)} \rightarrow Fe_{(s)}-C + Fe_{(s)}-O.$$

But this redox-type reaction may also occur on the next stable phase, Fe_3O_4, when it is considered that the thermodynamic data for both (bulk solids) equilibria are very similar (at 250°C):

$$Fe + CO \leftrightarrows FeO + C, \qquad \Delta G^\circ_{523} = 10.6 \text{ kcal}, \quad (1)$$

$$2\,Fe_3O_4 + CO \leftrightarrows 3\,Fe_2O_3 + C, \qquad \Delta G^\circ_{523} = 10.8 \text{ kcal}. \quad (2)$$

A gradual bulk carburization of iron oxide by CO and/or active C after its sequential reduction to Fe would be a parallel competitive reaction which decreases the amount (in the bulk) of the catalytically active phase (Fe_3O_4).

This scheme is confirmed by the hydrogen etching experiments of Fig. 2 which show that the initial fast decrease of the partial pressure of CH_4, which is accounted for by the interaction of H_2 with surface active carbon, is almost the same irrespective of the time on stream of the catalyst in the Fischer–Tropsch reaction (slow carburization and slow "polymerization" of carbon). Now, the next period of increasing and then decreasing partial pressure of CH_4, which is formed by the interaction between H_2 and "polymeric" carbon and iron carbide (*8*), reflects an increased fraction of the catalyst converted into inert material (integral of curves of Fig. 2 and Table 1) when the time on stream increases from 1.5 to 15 h (a maximum in these curves may be explained by the etching process of a solid inert phase by gaseous hydrogen). Simultaneously, the initial increase of the catalytic activity (Fig. 1) can be correlated with the conversion of α-Fe_2O_3 into the active phase Fe_3O_4 (Table 1) which finally disappears by sequential reduction and carburization and coverage by inactive carbon, causing also a decrease in the activity (Fig. 1). It is indeed shown that in the case of Fe_2O_3/SiO_2 preoxidized aerogel catalysts their very high and stable activity is paralleled with the presence of Fe_3O_4 and the absence of iron carbide in the spent catalyst (*2*).

2. *Catalyst B* (α-*Fe*)

The kinetic behaviour in the formation of methane of this prereduced catalyst is shown in Fig. 4. The selectivities into various alkanes are roughly the same as those observed for a nonreduced catalyst (*1*). The initial high activity in the formation of methane (Fig. 4, point a) almost immedi-

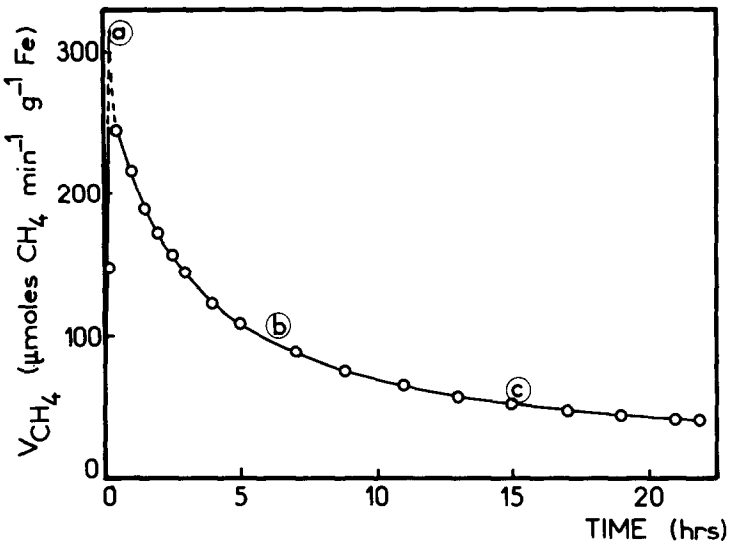

FIG. 4. Catalyst B (α-Fe). Rate of formation of CH_4 in the Fischer–Tropsch conversion as a function of time on stream (in micromoles of CH_4 per minute and per gramme of initial Fe).

ately decreases (b) and is lower after 15–20 h (c) than for the unreduced catalyst (Fig. 1c). It is difficult to find a basis for the comparison of activities of both catalysts, as the first is nonreduced and the second reduced. Moreover, it has been shown (*1*) that an attempt at the titration of zerovalent iron in the catalysts described here failed because all the zerovalent surface iron does not chemisorb CO at 25 or at −195°C, and also because ionic iron, too, is a site for chemisorption of CO. Thus (i) the irreversible chemisorption of CO is not specific for zerovalent iron and (ii) the nature of the active surface at, say, the pseudo-stationary state of catalysis (after 15 or 20 h) is not known. A rough comparison can be made on the basis of the surface area. The initial surface area of catalyst A is 90 m^2/g (*1*) and 43 m^2/g after 20 h of reaction; those of catalyst B are, respectively, 30 and 21 m^2/g. The activities per unit area, after 20 h of reaction (Figs. 1 and 4), are therefore 3.25 and 1.90 μmol min^{-1} m^{-2}. The unreduced catalyst (A) may therefore be considered as more active than the reduced catalyst (B) on the normalized surface area basis. The same type of conclusion but based on straightforward results is achieved for the aerogel catalysts (*2*).

The total carbon content as revealed by the CH_4 formed through H_2 etching of catalyst B (Table 3) is higher after 1 h of reaction (1.08 mol of CH_4 per gramme of initial iron) compared with the carbon content (0.24) observed after a comparable time on stream (1.5 h) on the unreduced catalyst A (Table 1). The bulk composition (XRD), given in Table 3, shows that α-Fe is easily converted to iron carbide ($Fe_{20}C_9$) whereas the surface composition (XPS) accounts for a high concentration of surface noncarbidic carbon. A greater part than previously (unreduced catalyst) of this surface carbon is inactive in Fischer–Tropsch synthesis. Indeed, the comparison of H_2 etching experiments of Figs. 2 and 5 shows that the rate of consumption of active carbon with the formation of methane (the fast initial decrease of p_{CH_4}) is smaller for the reduced catalyst B (curve a of Fig. 5) after 1 h of Fischer–Tropsch conversion than for the unreduced catalyst (curve a of Fig. 2) after a comparable time on stream (1.5 h). Though the total surface concentration of carbon (active and inactive), as revealed by XPS, already after

TABLE 3

Surface and Bulk Composition of Catalyst B (α-Fe)

Time on stream of the Fischer–Tropsch reaction (Fig. 4)	Surface composition (XPS)[a] (arbitrary units)		Structure (XRD)	Hydrocarbons formed by H_2 etching (moles of CH_4 per atom of initial Fe)		
				250°C	500°C	Total
	Fe	C				
15 min	1 (710.2)	4.4 (284.9)	*α-Fe*[b] $Fe_{20}C_9$			
1 h				1	0.08	1.08
10 h	1 (710.4)	3.5 (284.7)	$Fe_{20}C_9$			
24 h	1 (710.7)	2.83 (284.6)	$Fe_{20}C_9$	1.09	0.09	1.17

[a] The first number is related to the concentration, arbitrarily fixed to 1 for the iron and calculated by using cross sections published in Ref. (*5*). The number in parentheses represents the binding energy in electron volts.

[b] The most abundant phase is italicized.

15 min of conversion or after 10 h, is higher on the reduced catalyst B (Table 3) than on the unreduced catalyst A (Table 1), a simultaneous comparison of the catalytic activity of both catalysts (Figs. 1 and 4) shows that the reduced catalyst exhibits lower activity in the Fischer–Tropsch conversion than the unreduced catalyst. Clearly, a smaller fraction of surface carbon on the reduced catalyst is active in the Fischer–Tropsch synthesis. This behaviour also shows that the reduced catalyst is more efficient in the dissociation of CO into carbon but simultaneously it favours the transformation of ac-

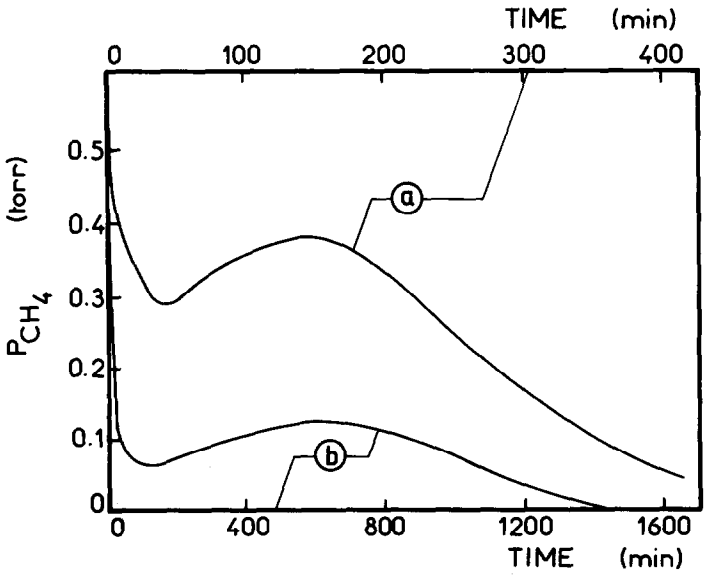

FIG. 5. Hydrogen etching forming methane at 250°C of catalyst B (α-Fe) after Fischer–Tropsch conversion during 1 h (curve a) and 10 h (curve b).

tive carbon into inactive carbon. A slower consumption of iron carbide ($Fe_{20}C_9$) by hydrogen etching (Fig. 5) as compared to the consumption of the carbide (χ-Fe_2C) formed in the unreduced catalyst (Fig. 2), as shown by the second part (with a maximum) of the curves in Figs. 2 and 5, probably accounts for a smaller activity in CH_4 formation of the first carbide. The reasons for these differences in activity toward H_2 etching of the two carbides are still unknown. They have to be paralleled with the higher activity toward atmospheric oxygen of the unreduced spent catalyst (A) containing χ-Fe_2C etched by hydrogen at 250°C (see above).

Table 4 also shows that for the reduced catalyst B after Fischer–Tropsch conversion during 5.5 h the ratio C/Fe before etching by argon ions is higher than that for the unreduced catalyst A (Table 2) and decreases also with the number of etchings. Simultaneously, the binding energy of surface carbon [graphitic and bonded to hydrogen, 284.2 to 284.8 eV (*10*)] decreases to the value corresponding to that of carbon in iron carbide [283.2 to 283.4 eV (*10*)]. The incorporation of carbon in the form of iron carbide is therefore also confirmed for the reduced catalyst B. The surface iron in the reduced catalyst is then the initial agent of the formation of active (and also of inactive) surface carbon, probably by the redox type of reaction with the dissociation of CO (*13, 14*), but with less efficiency than Fe_3O_4 (after the initial reduction by CO + H_2 of Fe_2O_3 into Fe_3O_4) in the unreduced catalyst

TABLE 4

Surface Composition of Catalyst B after 5.5 h in Fischer–Tropsch Conversion as Revealed by XPS before and after Etching by Argon Ions

Number of etchings	C/Fe calculated as in Table 2	C 1*s* binding energy (eV)
0	3.5	284.8
1	0.7	284.8, 283.4
2	0.18	284.2, 283.2

(compare Figs. 1 and 4), probably because α-Fe favours also the transformation of active into inactive carbon and also the carburization of iron. The sequence of steps occurring with the reduced catalyst during the Fischer–Tropsch synthesis seems therefore to differ from the sequence imagined for the unreduced catalyst. There is no fast initial bulk reduction of the catalyst which is already in the form of α-Fe. This accounts for the initial activity of the reduced catalyst (Fig. 4) being much higher than that of the unreduced catalyst (Fig. 1) which must be first converted to Fe_3O_4. The redox-type surface reaction between iron and CO leaves carbon which is active in the Fischer–Tropsch synthesis but also in the formation of iron carbide which is not a catalyst. Besides, this active carbon is readily transformed into inactive carbon in the presence of reduced iron. Iron carbide is formed to a higher extent on the reduced catalyst (compare Tables 1 and 3) and as it cannot be the partner in the redox-type reaction (whereas Fe_3O_4 and Fe seem to have this property) its formation is detrimental to the catalytic activity.

These results tend to show that the redox-type reaction between the catalyst and CO (*6*) which is dissociated (*13, 14*) leaving surface carbon, *active* in the Fischer–Tropsch synthesis (*7*), produces more carbon of this type if the solid partner is Fe_3O_4 rather than if it is α-Fe. Also the reaction path consuming this active carbon and giving the inactive iron carbide is longer when starting with Fe_3O_4 than with α-Fe (*12*). Finally the transformation of active into inactive carbon (noncarbidic) is also less intense on Fe_3O_4 than on α-Fe. These observations are verified in a straightforward manner in the case of oxidized Fe_2O_3/SiO_2 aerogel catalysts (*2*). Summing up, the present experiments show that when in the initial stages of reaction iron is reduced to α-Fe, the proportions of carbide (noncatalyst) and of total carbon formed during the Fischer–Tropsch synthesis are higher than those for the unreduced catalyst, but the

amount of surface active carbon, which is the intermediate in the formation of alkanes, is smaller. The reduced catalyst probably has a higher aptitude to promote the reaction $nC_{(active)} \rightarrow C_{n\,(inactive)}$ and also offers a shorter path to the carburization (*12*). This last property explains why even after 15–24 h in the stream the unreduced catalyst A and the reduced catalyst B are in different chemical states.

ACKNOWLEDGMENTS

We thank Professor C. O. Bennett (University of Connecticut, Storrs) for helpful discussions and some experimental contributions and B. Pommier for his technical contribution. This work was supported by a NATO grant for joint research.

REFERENCES

1. Reymond, J. P., Pommier, B., Mériaudeau, P., and Teichner, S. J., *Bull. Soc. Chim. Fr.* **1,** 173 (1981).
2. Blanchard, F., Reymond, J. P., Pommier, B., and Teichner, S. J., to be published.
3. Amelse, J. A., Butt, J. B., and Schwartz, L. H., *J. Phys. Chem.* **82,** 558 (1978).
4. Niemantsverdriet, J. W., Van Der Kraan, A. M., Van Dijk, W. L., and Van Der Baan, H. S., *J. Phys. Chem.* **84,** 3363 (1980).
5. Scofield, J. H., *J. Electron Spectrosc. Relat. Phenom.* **8,** 129 (1976).
6. Reymond, J. P., Mériaudeau, P., Pommier, B., and Bennett, C. O., *J. Catal.* **64,** 163 (1980).
7. Dwyer, D. J., and Somorjai, G. A., *J. Catal.* **52,** 291 (1978).
8. Matsumoto, H., and Bennett, C. O., *J. Catal.* **53,** 331 (1978).
9. Raupp, G. B., and Delgass, W. N., *J. Catal.* **58,** 361 (1979).
10. Bonzel, H. P., and Krebs, H. J., *Surf. Sci.* **91,** 499 (1980).
11. Johanson, L. I., Hagstrom, A. L., Jacobson, B. E., and Hagstrom, S. B., *J. Electron Spectrosc. Relat. Phenom.* **10,** 259 (1977).
12. Szendrei, T., and Van Berge, P. C., *Thermochim. Acta* **44,** 11 (1981).
13. Ponec, V., and Van Barneveld, W. A., *Ind. Eng. Chem. Prod. Res. Dev.* **18,** 269 (1979).
14. Wedler, G., and Korner, H., *Ber. Bunsenges. Phys. Chem.* **85,** 283 (1981).